

Selective study of polymer/dielectric interfaces with vibrationally resonant sum frequency generation via thin-film interference

Philip T. Wilson, Kimberly A. Briggman, William E. Wallace, John C. Stephenson, and Lee J. Richter^{a)}

National Institute of Standards and Technology, 100 Bureau Drive, Gaithersburg, Maryland 20899-8372

(Received 14 December 2001; accepted for publication 4 March 2002)

A technique for selective characterization of the structure of free and buried thin-film interfaces by vibrationally resonant sum frequency generation spectroscopy is described. Manipulation of Fresnel coefficients by choice of film thickness on a reflecting substrate allows simultaneous optimization of the signal from the desired interface and minimization of the signal from other interfacial sources. This technique is demonstrated for the free polystyrene (PS)/air and the buried PS/spin-on glass interfaces. Our spectra show that the pendant phenyl group orientation is similar at the buried and free interfaces, with the phenyls pointing away from the bulk PS at each interface.

[DOI: 10.1063/1.1475358]

Surfaces and interfaces are critical to the functional properties of many polymer applications including the adhesion of polymer coatings for electronic packaging and optical fibers, biocompatibility of medical devices, the structural integrity of polymer composites, and the formation of lamellae in block copolymers. Polymer interfaces can differ considerably from the bulk in important characteristics such as glass transition temperature, end-group concentration, molecular weight distribution, amorphous/crystalline ratio, and crosslink density.¹

Optical measurements of polymers are advantageous as they are nondestructive, noncontact, and can be performed in almost any ambient. However, buried interfaces are difficult to study by conventional linear spectroscopies due to the dominance of the signal from the bulk material. Vibrationally resonant sum frequency generation (VR-SFG) has emerged as a powerful tool for the study of the molecular structure of interfaces.² As a second-order nonlinear optical interaction, VR-SFG has inherent interface specificity; signals from centrosymmetric bulk regions are symmetry forbidden in the electric dipole approximation. Additionally, VR-SFG has the advantage, with respect to linear optical techniques, that it can determine both the orientation of functional groups at a surface and their alignment. Recently, VR-SFG has been applied to the study of the free surfaces of polymers, providing insight into surface structure,³ chemical composition,⁴ and processing.⁵

To study a particular buried interface in a multilayer system, its signal must be distinguished from that of other interfaces in the system. We have developed a thin-film interference technique that allows the study of buried interfaces between any two dielectric films, independent of dielectric constant. In this work, the two materials of interest are deposited as optical quality thin films on a highly reflecting

substrate. The top film is polystyrene (PS) and the bottom film is a hydrogen silsesquioxane spin-on glass (SOG) on a gold (Au) substrate. The thicknesses of the two films are chosen to provide selective enhancement via constructive optical interference of VR-SFG generated in transmission and in reflection from the interface of interest: either the free surface of the top film, or the buried interface between the top and bottom films. Additional contrast is achieved by designing the film stack so that the other interface is effectively nulled through destructive interference.

For planar thin-film systems within the electric dipole approximation, the outgoing electric field generated at the sum frequency by a single interface can be expressed in terms of the incident electric fields of the resonant infrared (IR) and nonresonant visible (VIS) laser beams:

$$E_t(\omega_{\text{SUM}}) = F_{ii}^{\diamond}(\omega_{\text{SUM}})\chi_{ijk}^D(\omega_{\text{SUM}} = \omega_{\text{VIS}} + \omega_{\text{IR}})F_{jm}(\omega_{\text{VIS}})E_m(\omega_{\text{VIS}})F_{kn}(\omega_{\text{IR}})E_n(\omega_{\text{IR}}), \quad (1)$$

where E is the electric field vector of the IR, VIS, and sum frequency (SUM) beams, χ is the interface nonlinear susceptibility, F is the conventional Fresnel factor relating the electric field at the interface to the incident field, and F^{\diamond} is a nonlinear Fresnel factor, accounting for both the directly transmitted and reflected components of the outgoing SUM beam. F can be readily calculated for an arbitrary multilayer system using transfer matrix techniques.⁶ F^{\diamond} can be calculated via many schemes;⁷ we have used the Green's function method of Sipe.⁸ χ , in general, contains 27 elements. For films that are isotropic in the plane of the surface ($C_{\infty v}$ symmetry about the surface normal, z), there are only four distinct nonvanishing elements, $ijk = zzz$, $zxx = zyy$, $xzx = yzy$, and $xxz = yyz$. The *ssp* polarization combination, in which $E(\omega_{\text{SUM}})$ and $E(\omega_{\text{VIS}})$ are polarized perpendicular and $E(\omega_{\text{IR}})$ is polarized parallel to the plane of incidence, probes χ_{xxz} exclusively. The *ssp* VR-SFG signal from a two-film stack can be expressed as:

^{a)} Author to whom correspondence should be addressed; electronic mail: lee.richter@nist.gov

$$\text{Signal} = \left| F_w^{\text{free}}(\omega_{\text{SUM}}, \omega_{\text{VIS}}, \omega_{\text{IR}}) \chi^{\text{free}} E(\omega_{\text{VIS}}) E(\omega_{\text{IR}}) + F_w^{\text{buried}}(\omega_{\text{SUM}}, \omega_{\text{VIS}}, \omega_{\text{IR}}) \chi^{\text{buried}} E(\omega_{\text{VIS}}) E(\omega_{\text{IR}}) + F_w^{\text{sub}}(\omega_{\text{SUM}}, \omega_{\text{VIS}}, \omega_{\text{IR}}) \chi^{\text{sub}} E(\omega_{\text{VIS}}) E(\omega_{\text{IR}}) \right|^2 \quad (2)$$

where F_w is the product $F_{xx}^\diamond(\omega_{\text{SUM}}) F_{xx}(\omega_{\text{VIS}}) F_{zz}(\omega_{\text{IR}})$ and contributions arise from all three interfaces: air/PS, PS/SOG, and SOG/Au. In general, F_w is a complex number and a complicated function of the three frequencies and angles of incidence. For the case of VR-SFG on submicron thin films, the behavior is simplified: the IR wavelength is long compared to the film thickness, so $F(\omega_{\text{IR}})$ is approximately constant. The VIS and SUM wavelengths are sufficiently close that $F^\diamond(\omega_{\text{SUM}})$ and $F(\omega_{\text{VIS}})$ behave similarly.

The experiments used a SFG apparatus described previously.⁹ Broad-bandwidth ($>150 \text{ cm}^{-1}$ full width at half maximum) $3 \mu\text{m}$ IR pulses, derived from a $\sim 100 \text{ fs}$, 1 kHz , regeneratively amplified Ti-Sapphire laser system, are temporally and spatially overlapped with narrow-bandwidth ($\sim 3 \text{ cm}^{-1}$) 794 nm (VIS) pulses at the sample. The reflected SUM light is collected, dispersed in a 0.75 m spectrograph, and detected with a scientific grade charge coupled device array detector. This allows the simultaneous acquisition of a $>300 \text{ cm}^{-1}$ wide SFG spectrum with approximately 3 cm^{-1} resolution. In this work, the IR and VIS pulse energies, beam diameters, and external angles of incidence were typically: $4 \mu\text{J}$, $100 \mu\text{m}$, 54° and $1 \mu\text{J}$, $150 \mu\text{m}$, 36° , respectively.

The SOG films were formed by spin coating Dow Corning FOx-14® (Ref. 10) at 2000 rpm from methyl isobutyl ketone solutions onto Au films ($\sim 200 \text{ nm}$ thick) evaporated onto Si wafers with a Cr adhesion layer. The SOG films were annealed at 300°C in air for 1 h . The polymer thin films were $220\,000$ number-average relative molecular mass atactic PS, spin coated on the SOG at 2000 rpm from toluene solutions and annealed under a vacuum for 2 h at 120°C . Spectrometric ellipsometry determined the PS and SOG film thicknesses with $1\text{--}2 \text{ nm}$ accuracy. Atomic force microscopy studies of the glass prior to deposition of the PS determined a root-mean-square (rms) roughness of $1.0\text{--}1.5 \text{ nm}$, while studies of the PS free surface determined a rms roughness of $0.5\text{--}0.8 \text{ nm}$.

Shown in Fig. 1 are VR-SFG *ssp* spectra of a 129 nm thick film of PS deposited on films of SOG of varied thicknesses, on Au substrates. The principal vibrational resonances in the range 3000 to 3100 cm^{-1} can be attributed to the stretching vibrations of the CH bonds on the pendant phenyl groups of the PS.¹¹ The lines through the spectra shown in Fig. 1 are fits by a Levenberg–Marquardt algorithm to the form:

$$\text{Signal}_n = \left| B_n + C_n^{\text{free}} e^{i\varphi_n^{\text{free}}} \sum_{m=1}^7 \frac{A_m^{\text{free}}}{\nu - \nu_m^{\text{free}} + i\Gamma^{\text{free}}} + C_n^{\text{buried}} e^{i\varphi_n^{\text{buried}}} \sum_{j=1}^7 \frac{A_j^{\text{buried}}}{\nu - \nu_j^{\text{buried}} + i\Gamma^{\text{buried}}} \right|^2, \quad (3)$$

where n denotes the spectrum, (1–6), B accounts for the strong nonresonant SFG from the Au substrate, and both the free and buried interfaces are represented by seven resonant modes: five normal modes and two combination bands¹¹

modeled as Lorentzian oscillators with variable real amplitudes A and frequencies ν and a common width Γ . Because the SOG/Au interface contains no vibrational resonances in this frequency region, its contribution is included in B . The six spectra in Fig. 1 were simultaneously fit to the two constituent interfacial spectra with variable complex weight $C e^{i\phi}$. The phase for each interface is determined by the relative phase between the Au nonlinear susceptibility and that of the phenyl oscillator and by the optical delay between the two interfaces, which depends on film thicknesses.

The data points in Fig. 2 show the experimental fit results for the (a) phases, ϕ , and (b) weights, C , of the two constituent spectra for each of the six samples, plotted versus the measured SOG thickness. The lines show the magnitude and phase of the calculated Fresnel weights, F_w , for nonlinear sources localized at the free and buried interface scaled to the experimental data. The calculation used the known film thickness and index of refraction for each layer. The fit yielded phases and weights for the two spectra expected for the Fresnel factors of each film stack. The agreement between experiment and the calculation based on the Fresnel factors gives confidence that the data, which contains some contribution from each interface, have been correctly analyzed to reveal the unique spectra of the free and buried interfaces. Shown in Fig. 2(c) is the calculated contrast ratio between the buried and top interface SFG (*i.e.*, $F_w^{\text{buried}}/F_w^{\text{free}}$ for *ssp* polarization). The heights, widths, and positions of the maxima in the contrast ratio depend on wavelength, angle of incidence, polarization, and index of refraction. For the properly chosen film thickness, these maxima exceed 100, with half widths of one to several nm

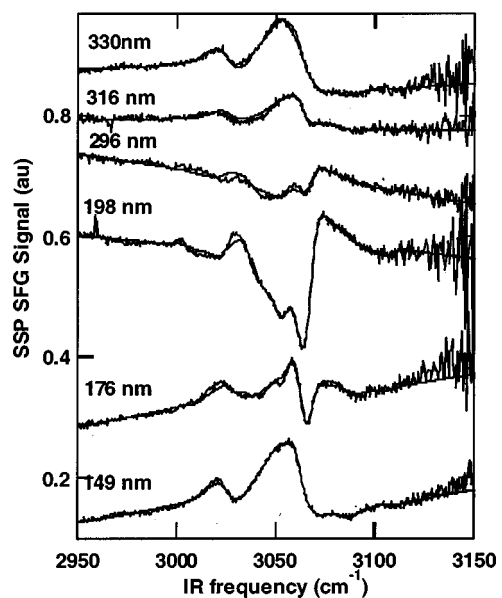


FIG. 1. VR-SFG spectra, in the *ssp* configuration, of $\sim 129 \text{ nm}$ PS films deposited on SOG films of indicated thicknesses vertically displaced for clarity. The smooth lines are fits to the model form as described in Eq. (3).

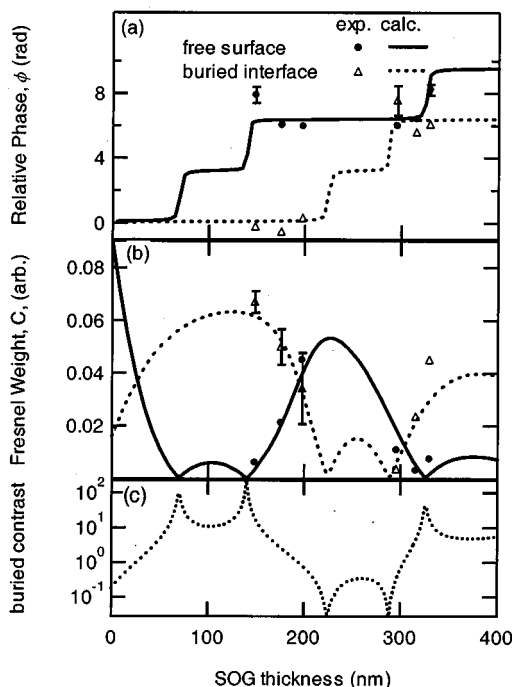


FIG. 2. Comparisons of the calculated combined Fresnel weight F_w , with the fit (a) phase, ϕ , and (b) amplitude, C , of the free surface and buried interface contributions to the spectra in Fig. 1. (c) Calculated buried interface to free surface Fresnel weight contrast ratio, $F_w^{\text{buried}}/F_w^{\text{free}}$. Error bars not shown are comparable to or smaller than the size of the data symbol.

thickness. The calculations suggest that this SFG technique with optimized film thicknesses allows selective measurement of a single interface. Measurement at variable incident angles as is common in ellipsometry would relax the stringent requirements on sample preparation.

Figure 3 shows the spectra for the samples with a (b) 198 nm SOG film and a (c) 330 nm SOG film as the bottom layer with 129 nm PS layer on top, which are the best exem-

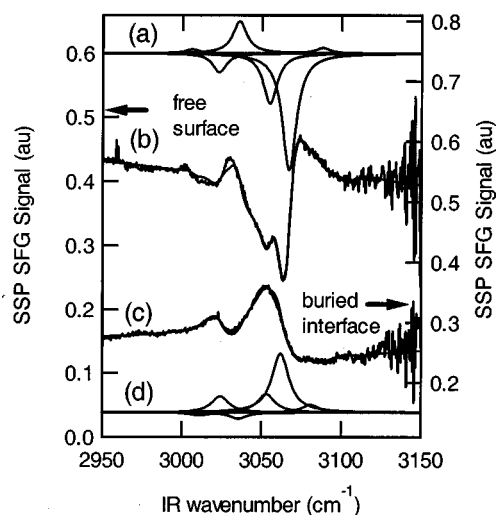


FIG. 3. The spectra for a 129 nm PS film on a (b) 198 nm SOG film (dominated by the free surface contribution) and on a (c) 330 nm SOG film (dominated by the buried interface contribution). The line through the data is the fit to the complete model. The individual resonance features are the imaginary part of the Lorentzian components of the fits to the dominant (a) free or (d) buried interface.

plars of the free and buried interfaces, respectively. The components of the fits for the pure (a) free and (d) buried interfaces are also shown. The two spectra differ in the sign of the peaks relative to the nonresonant background. This difference is not due to differences in ϕ of the Fresnel factors; as shown in Fig. 2, this phase is the same ($\sim 2\pi$) for the free surface with 198 nm SOG and the buried interface with 330 nm SOG. Rather, it is due to differences in the phase of the vibrational resonances that arise because of the orientation of the phenyl groups at the free and buried interfaces is in opposite directions with respect to the Au surface. Previous measurements of the free surface have determined that the phenyl groups point out of the bulk of the film and away from the nonresonant substrate.¹¹ Therefore, a change in the phase of the vibrational resonances at the buried interface suggests that the phenyl groups at the buried interface must point away from the PS film toward the SOG/Au substrate. The frequencies of the phenyl CH stretch modes are ~ 5 cm^{-1} lower in frequency for the buried interface than the free surface. There is a slight increase in the linewidth Γ for the buried interface (6.5 ± 0.5 cm^{-1}) with respect to that of the free surface (5.3 ± 0.5 cm^{-1}). The frequencies and linewidths of vibrations at the buried interface are more similar to the PS bulk than are those at the free surface, which are at higher frequencies and narrower than the bulk vibrations. The similar relative amplitudes of the components in the spectra of the two interfaces suggest that the orientational distribution of the buried interface is nearly identical to that previously measured for top surfaces.¹¹ The similarity between the free surface and the buried PS/SOG interface is in contrast to the very different orientational distribution recently observed for the PS/sapphire interface via total internal reflection SFG.¹² This is likely due to a reconstruction of the PS/dielectric interface that can be driven by the higher surface energy of sapphire with respect to the SOG.¹³

¹D. Briggs, *Surface Analysis of Polymers by XPS and Static SIMS*, (Cambridge University Press, Cambridge, U.K., 1998).

²P. B. Miranda and Y. R. Shen, *J. Phys. Chem. B* **103**, 3292 (1999); G. L. Richmond, *Anal. Chem.* **69**, A536 (1997); C. D. Bain, *J. Chem. Soc., Faraday Trans.* **91**, 1281 (1995).

³X. Wei, S.-C. Hong, X. Ahuang, T. Goto, and Y. R. Shen, *Phys. Rev. E* **62**, 5160 (2000).

⁴Z. Chen, R. Ward, Y. Tian, S. Baldelli, A. Opdahl, Y. R. Shen, and G. A. Somorjai, *J. Am. Chem. Soc.* **122**, 10615 (2000); Z. Chen, R. Ward, Y. Tian, A. E. Eppler, Y. R. Shen, and G. A. Somorjai, *J. Phys. Chem. B* **103**, 2935 (1999).

⁵D. Kim and Y. R. Shen, *Appl. Phys. Lett.* **74**, 3314 (1999); D. Zhang, S. M. Dougal, and M. S. Yeganeh, *Langmuir* **16**, 4528 (2000).

⁶P. Yeh, *Optical Waves in Layered Media* (Wiley, New York, 1988).

⁷D. S. Bethune, *J. Opt. Soc. Am. B* **6**, 910 (1989); *ibid.* **8**, 367 (1991); N. Hashizume, M. Ohashi, T. Kondo, and R. Ito, *ibid.* **12**, 1894 (1995).

⁸J. E. Sipe, *J. Opt. Soc. Am.* **B4**, 481 (1987).

⁹L. J. Richter, T. P. Petralli-Mallow, and J. C. Stephenson, *Opt. Lett.* **23**, 1594 (1998).

¹⁰We identify certain commercial materials in this article to specify the experimental procedure. In no case does such identification imply recommendation or endorsement by the National Institute of Standards and Technology, or that the materials or equipment identified are necessarily the best available for the purpose.

¹¹K. A. Briggman, J. C. Stephenson, W. E. Wallace, and L. J. Richter, *J. Phys. Chem. B* **105**, 2785 (2001).

¹²K. S. Gautam, A. D. Schwab, A. Dhinojwala, D. Zhang, S. M. Dougal, and M. S. Yeganeh, *Phys. Rev. Lett.* **85**, 3854 (2000).

¹³L. J. Richter, P. T. Wilson, W. E. Wallace, J. C. Stephenson, and K. A. Briggman (unpublished).